JOURNAL OF FORENSIC SCIENCES

J Forensic Sci, March 2012, Vol. 57, No. 2
doi: 10.1111/j.1556-4029.2011.01973.x
Available online at: onlinelibrary.wiley.com

PAPER

ANTHROPOLOGY

Annamaria Crescimanno,[1,*] *M.S. and Sam D. Stout,*[2] *Ph.D.*

Differentiating Fragmented Human and Nonhuman Long Bone Using Osteon Circularity

ABSTRACT: Distinguishing between human and nonhuman bone is important in forensic anthropology and archeology when remains are fragmentary and DNA cannot be obtained. Histological examination of bone is affordable and practical in such situations. This study suggests using osteon circularity to distinguish human bone fragments and hypothesizes that osteons will more closely resemble a perfect circle in nonhumans than in humans. Standard histological methods were used, and circularity was determined using an image analysis program, where circularity was controlled for by Haversian canal measurements. Homogeneity was first tested for multiple variables within human and nonhuman samples. No significant differences were found between human sexes ($p = 0.657$) or among nonhuman species ($p = 0.553$). Significant differences were found among intraskeletal elements of both humans ($p = 0.016$) and nonhumans ($p = 0.013$) and between pooled samples of humans and nonhumans ($p < 0.001$). Results of this study indicate that osteon circularity can be used to distinguish between fragmented human and nonhuman long bone.

KEYWORDS: osteon, circularity, fragmented bone, nonhuman, differentiate, histomorphology, forensic

Distinguishing between human and nonhuman bone is important in forensic anthropology and archeology, especially when skeletal remains are fragmentary and DNA cannot be obtained because of poor preservation or high costs. When no identifiable macroscopic landmarks are visible, a histologically based determination may be the only alternative. Microstructural differences between human and nonhuman bones have been documented (e.g., plexiform bone and osteon banding) and are preserved in archeological specimens (1). Unfortunately, current methods, such as measuring differences in osteon size and number (osteon population density) in a section of bone, have yet to yield high success rates when using such bone microstructures to distinguish between human and nonhuman bone (2,3). Therefore, an alternative method for using bone microstructure is needed. This study compares the shape (circularity) of osteons, which are present in the bone of all large vertebrates.

The objective of this study was to compare osteon circularity between humans and three similarly sized mammals (*Canis*, *Sus*, and *Odocoileus*, or dog, pig and deer) to see whether human bone can be readily distinguished. Femur, humerus, and rib are sampled for each species to include major load-bearing long bones of the upper and lower extremity, as well as a less dynamically loaded bone not directly involved in locomotion. *Canis*, *Sus*, and *Odocoileus* were chosen for this study for three reasons: they are often encountered in forensic cases, in which nondiagnositc and small bone fragments are recovered (2); they are similar in size to humans, so their bone undergoes similar growth and remodeling as human bone (2–5); and they are among the most often described animal remains in archeological and forensic journals (4). The current study progresses in three steps: first, intraspecific comparisons by sex and bone are made within the human sample; next, nonhuman interspecific comparisons are made, and third, the nonhumans are compared with the human sample. This study hypothesizes that circularity will more closely approximate a perfect circle in nonhuman long bones than in human ones.

Because bone is a living tissue, it maintains itself throughout life via the metabolic process of remodeling. Remodeling takes place in six phases (activation, resorption, reversal, formation, mineralization, and quiescence) and is accomplished by bone resorbing (osteoclasts) and forming (osteoblasts) cells working together in a complex arrangement in which their appearance and activity are coordinated temporally and spatially to form what is commonly referred to as the basic multicellular unit (BMU) (6). This unit is a three-dimensional structure consisting of two separate components: a cutting cone and a closing cone. The cutting cone is lined with roughly 10 osteoclasts, whereas the closing cone is lined with hundreds of osteoblasts (6–8).

During the activation phase, in which the creation of a BMU is initiated, bone-lining cells withdraw and expose the surface of bone that will be resorbed. The secretion of cytokines (e.g., CSF-1) (9) induces osteoclast precursor cells to appear in the area of the exposed bone where they differentiate into mature osteoclasts. These mature osteoclasts resorb bone forming a bay or tunnel, known as a resorptive bay or cutting cone (10) that is 150–350 μm in diameter (11,12) in the exposed area of bone. The cutting cone progresses through the cortex of bone, at about 20 μm/day (6), in a direction associated with mechanical strain (12).

The resorption phase is complete, in about 3 weeks, after which apoptosis of osteoclasts occurs, attracting the cells of the closing

[1]Human Biology Department, University of Indianapolis, 1400 E Hanna Ave., Good Hall Room 008, Indianapolis, IN.
[2]Anthropology Department, The Ohio State University, 4052 Smith Laboratory, 174 W. 18th Avenue, Columbus, OH43210-1106.
[*]Present address: 249 W El Portal, #4, San Clemente, CA 92672.

Received 11 Aug. 2010; and in revised form 2 Dec. 2010; accepted 1 Jan. 2011.

cone to the freshly resorbed surface. During the reversal phase, that follows, the uneven periphery of the resorptive bay is smoothed by a group of mononuclear cells (11) to form what is known as a cement line (reversal line), which can be seen microscopically (6). The reversal phase represents the transition in which osteoblast activity replaces osteoclast activity in the region of resorbed bone and takes *c.* 1 month to complete. Some debate exists as to whether or not this area is highly mineralized (7,13,14).

During the formation phase that follows and lasts for 3 months, the osteoblasts lining the closing cone are signaled by various hormones and chemicals to deposit an organic matrix composed of Type I collagen, proteoglycans, water, and noncollagenous proteins referred to as osteiod (6). Osteiod mineralizes in *c.* 10–15 days and is organized into concentric lamellae as it becomes mineralized by the deposition of crystals of hydroxyapatite-like inorganic calcium phosphate (6,8). The last phase of BMU creation is quiescence during which osteoblasts either flatten onto the newly laid bone to become bone-lining cells that regulate the calcium balance between serum and bone tissue or they become trapped in the matrix they form to become the ubiquitous bone cells called osteocytes (6,7). This complete remodeling process, which takes 3–4 months, results in a bone structural unit (BSU), which in cortical bone is called a secondary osteon (6–8,13).

In transverse section, secondary osteons appear as about five to eight concentric rings made up of Haversian lamellae (6,7,13). In human compact bone, secondary osteons average 300 μm in diameter by 300–400 μm in length (6,15) and form parallel to the long-bone axis. The outermost layer of each secondary osteon is marked by the cement (reversal) line (2,6). Within each osteon is a circular pathway, or Haversian canal, for blood, lymph, and nerves. Each Haversian canal connects to another by a Volkmann canal, which moves through the bone at different angles and creates a network within the bone (6,16).

Robling and Stout (8) recognize four types of secondary osteons (Fig. 1). Type I, also called common osteons, usually have uninterrupted, concentrically deposited lamellae that surround a centrally located Haversian canal. Type II, or embedded osteons, form within common osteons but do not cross the cement line of the existing secondary osteon within which they form. Type II osteons usually form owing to the erosion of an existing Haversian canal that is followed by concentric deposition of Haversian lamellae. Type III, or double zonal osteons, form in the same way as common osteons but experience an interruption during the formation of the BMU and which results in a hypercalcified ring within the osteon. Finally, Type IV, or drifting osteons, are BSUs that experience simultaneous resorption and formation on opposite sides of the resorptive bay. The osteon becomes elongated in a transverse section as if it is "drifting" through the bone. The end result is a Haversian canal with four to eight concentric lamellae with one side experiencing a tail of deposited lamellae. Robling and Stout (8) report that drifting osteons do not follow the mechanical loading strain that Type I osteons do and are most commonly observed in specimens representing the first 10 years of life; they can occupy up to 53% of the resorption space in subadult rib cortices. By the eighth decade of life, however, Type IV osteons drop to only 8%, which indicates an inverse relationship between age and the frequency of drifting osteons. Because of the manners in which Type III–Type IV osteons form, they are excluded in this study, so only Types I and II are considered.

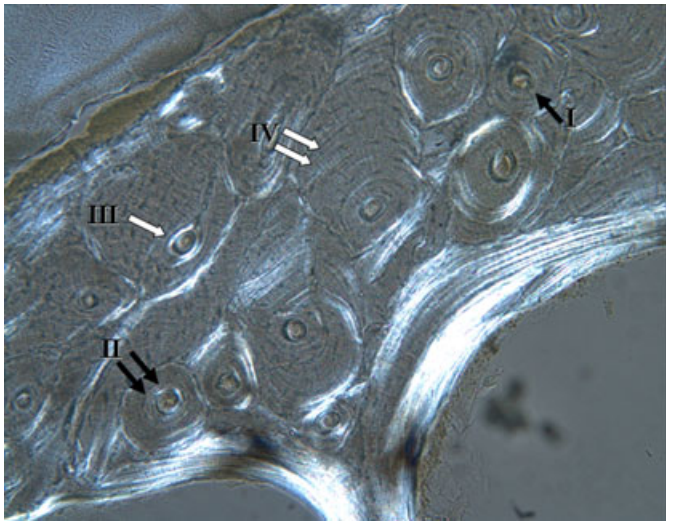

FIG. 1—*Digital photograph from the cortex of a human rib illustrating the four types of osteons: single arrow indicates Type I (normal) osteon, double arrows indicate Type II (embedded) osteon, single-open arrow indicates Type III (double zonal) osteon, and double-open arrows indicate Type IV osteon (drifting). 120×.*

Human Bone Microstructure

In a cross section of a typical adult human long bone, circumferential lamellae bone is present at the periosteal and endosteal margins, with osteons scattered in between. The dense middle portion of bone consists of roughly 50% secondary osteons and 50% interstitial lamellae. The secondary osteons may appear as completely formed, with a Haversian canal surrounded by concentric lamellae and cement line, or as remnants of osteons (osteon fragments) that have become partially replaced through the process of remodeling or resorption by another more recent osteon (2).

Variation exists in osteon histomorphology and histomorphometry within and between human bones. For example, in ribs, osteon population densities show little variation but the actual size of each osteon varies greatly (17). Differences in osteon diameter, Haversian canal diameter, and total osteon area have also been reported between ribs and femora (18).

Age is another variable to consider when looking at variations in osteon size, shape, and number. Because of the relatively rapid appositional growth in subadults, periosteal circumferential lamellar bone (primary bone) is more abundant at the endosteum. As individuals age, osteons replace periosteal primary lamellae, while endosteal lamellae are resorbed by endosteal expansion. Also with age, osteons become smaller and more numerous at the periosteal surface than at the endosteal surface and become more "fragmented" as bone remodels throughout life; nonhumans exhibit the same aging trends (2). Both human males and females also are said to exhibit a significant increase in total Haversian canal area and number with increasing age (19). Age also significantly relates to and positively correlates with osteon circularity and area, and osteon diameter differs significantly between sexes (20).

Sex can affect osteon number and size in humans (20–22). In certain archeological populations, females have been reported to exhibit smaller Haversian canals and larger osteons than males, in femoral cross sections (21), and average osteon diameter and area were reported to be significantly different between the sexes in other archeological populations (22). It has been reported elsewhere that, when compared to females, males have more osteons (20) and females have a *larger* mean Haversian canal area than males do at similar ages (19,20). Further confusing matters, there have also been reports of no sex-based differences for total osteon area and Haversian canal area (23). These contradictory results may reflect

differences in modern and archeological populations, how osteons are defined and measured, and in varying sample size among the studies.

Nonhuman Bone Microstructure

Dog

Mature dog long bones exhibit mostly dense Haversian bone with osteons that are similar in size, having three to five lamellae rings, and small Haversian canals relative to osteon size (4). Circumferential bone is present and well developed on both the endosteal and periosteal surfaces of bone but with a few osteons scattered throughout (2). It has been reported that osteons that are maturing, or forming, tend to do so at a consistent rate among all dog long bones (24) but that the total number differs significantly between sites of one bone and between different long bones (25). Number of osteon canals is not reported to be significantly different among ribs or between sides of the same dog (25).

Variation in the diameter of osteons does exist between male and female dogs; males exhibit a greater diameter than females, yet females exhibit a higher total number of osteons (26). Lactating females are reported to have higher rates of bone remodeling, in the femur, which contribute to the differences seen in total osteon number between the sexes (5).

Haversian canal density in femoral diaphyses of dogs has been reported to be greater when compared to human Haversian canal density, but with considerable overlap (27). A large range in Haversian canal density for dogs has been reported (28) too, meaning that the overlap between these ranges does not make Haversian canal density suitable for distinguishing human from nonhuman bone fragments. However, osteon diameter of dogs is suggested to be significantly smaller than that of humans, which is promising for differentiating between the two (27).

Pig

Two histomorphological features, plexiform bone and osteon banding, often make pig bone easily distinguishable from human bone (5). Plexiform bone is formed by circumferential, longitudinal, and radial primary osteons and results in a ''brick wall'' appearance that contains rectangular vascular spaces within it (2). Although there may be subtle differences, many consider laminar, and fibrolamellar, to be synonymous with plexiform (13). Plexiform bone can also have layers of lamellar bone that alternate with bone tissue containing osteonal banding (29). Such banding appears near the endosteal surface as two or three rows, each containing five to 20 primary osteons (2). In an immature pig, plexiform bone is very abundant throughout the cortical bone, especially in large animals whose bones need to grow in diameter quickly (13). Mature pig long bones show almost no osteon banding but mostly plexiform bone with dense Haversian bone at the posterior aspect (2) and few osteons in the periosteum (30). Mature pigs' osteons exhibit medium-sized Haversian canals overall (2). Depending on which area of the bone a fragment is from, it may become difficult to distinguish between pig and human bone histologically, because secondary osteon population density is reportedly higher, especially in wild boar (31).

Deer

Like humans, deer experience different amounts of osteonal bone throughout life but unlike humans they also experience varying amounts of plexiform bone (32). In newborn and fetal deer, the primary bone is plexiform and consists of avascular areas. In immature deer, Haversian bone is found at the endosteal surface, while the majority of plexiform bone occurs near the periosteal surface (2). Most osteons observed are primary, scattered throughout the plexiform bone, and similar in shape and size with little interstitial lamellar bone between (32). Mature deer long bone exhibits a thin layer of circumferential lamellae bone around the whole periosteal surface. Besides this layer, the mature bone is largely Haversian bone, most prominently seen at the endosteal surface and posterior area of bone (2).

Human and Nonhuman Microstructure Comparison

Recently, researchers have looked at the microscopic differences between human and nonhuman bone but have found very little to successfully differentiate between the two (2,3). On the other hand, Martiniakova et al. (33) report that differences in osteon and Haversian canal area, perimeter, and minimum diameter do exist between humans and nonhumans, as well as between different nonhuman species. Those authors developed a predictive model to distinguish between the long bones of cows, rabbits, pigs, sheep, and humans, with a 76.17% success rate in classification using osteon and Haversian canal area, perimeter, and minimum osteon diameter. In a similar study, Martiniakova et al. (34) report that the perimeter and minimum diameter of primary Haversian canals were the most discriminating variables. The authors recommend that 50–100 osteons be measured when using their model (33), but this procedure may be difficult with fragmented remains.

The most commonly reported difference between human and nonhuman bone is the presence of plexiform bone in nonhumans (3,33). Morris (4) conducted a study on a total of 50 long bone elements from dog, pig, and deer and reported that only 16.7% of mid-thoracic ribs and 64% of long bones had plexiform bone present. Deer and pig had the highest percentages. Plexiform bone is usually absent in humans, except for rare cases when children experience large growth spurts (3), but because it is not always found in animals it should not be used alone for differentiation.

Osteon banding has been cited as a differentiating tool (2,3,29,35). According to Watson and McClelland (35), osteons in human cortical bone are scattered and evenly spaced, whereas in many animals, osteons tend to align in rows or form plexiform bone. Although these characteristics indicate animal bone, Ubelaker (36) cautions that considerable variety exists between species and between bones of the same animal, which can make identification difficult. Because areas within the cortical bone of all of these species contain regions composed of varying amounts of osteonal bone, and considerable overlap exists for osteon dimensions, distinguishing fragments of their bone from human is often not possible based upon osteon size or density alone.

Osteon circularity is reported to be higher in nonhumans than humans for specific skeletal elements, especially in areas of bone under high strain (2). This trend has been seen in mule deer calcanei (37) and radii of standard-breed horses (2). Based on this research and the loading mechanics of human and nonhuman bone, the authors believe that nonhuman osteons will be more circular overall than human osteons. We propose using a shape variable, circularity, to provide a greater ability to distinguish human bone fragments histologically, where osteon circularity will more closely resemble a perfect circle in nonhumans than in humans. To explore this, several aspects of osteon circularity must first be explored and include the degree of intraskeletal, intraspecies, and interspecies variability for osteon circularity.

TABLE 1—*Sample distribution by species, bone type, and sex.*

Species	Femur	Humerus	Rib	Total
Human	14	14	13	41
Male	7	7	7	21
Female	7	7	6	20
Canis (Dog)	5	5	5	15
Sus (Pig)	5	4	5	14
Odocoileus (Deer)	5	5	5	15
Total human	14	14	13	41
Total nonhuman	15	14	15	44
Combined	29	28	28	85

Materials and Methods

Fourteen cadavers from the Biology Department at the University of Indianapolis were used to collect human skeletal elements. The sample consisted of seven European-American females and seven European-American males ranging in age from 54 to 78. A mid-shaft sample from the right humerus, right femur, and right fourth rib of each cadaver was collected, bagged, and labeled (Table 1). Nonhuman skeletal elements were obtained from five *Canis*, five *Sus*, and five *Odocoileus* ($n = 15$) (Table 1). A mid-shaft sample was taken from a humerus, femur, and rib of each. Epiphyses of all long bones were present and fused, suggesting that all dog, pig, and deer were sexually mature. *Canis* samples were collected from five medium-sized dogs, at the mid-shaft of the right femur, humerus, and rib, but sex and age were not equally represented. Mid-shaft bone samples of the deer and pig were obtained at different times from a local meat locker; therefore, a rib, femur, and humerus were not always collected from a given animal.

Samples were prepared for microscopic analysis using standard histological methods (38). All rib samples were embedded in Epo-Kwick plastic resin (Buehler Ltd., Lake Bluff, IL) because of the thinness of the cortical bone and left to cure for at least 24 h in a fume hood. Humeral and femoral samples did not require embedding. Using a low-speed gravity-feed isometric saw, Isomet 1000 Precision Saw (Buehler Ltd.), each sample was then sectioned in a transverse plane, at the measured bone mid-shaft, to produce *c.* 500-μm-thick parallel-sided bone wafers (Buehler Ltd). Each sample was mounted onto a slide using Permount glue (Fisher Scientific Ltd., Nepean, Ontario, Canada), a clear mounting agent, and left to dry for at least 2 days in a fume hood. Samples were then ground by hand, first with 220-grit sand paper, then polished with 600-grit sandpaper to a final thickness of *c.*100 μm, and cleaned with xylene. Cover slips were not used.

Each slide was examined at a magnification of 20× using transmitted light microscopy. Three fields, each containing at least one osteon, were viewed from the anterior, posterior, medial, and lateral areas of each wafer (Fig. 2) for a total of 12 circularity readings (12 osteons) per bone. All fields were digitally photographed with the aid of a digital camera and the images transferred into an image analysis software program where a digitizing tablet and stylus were used for manually outlining each osteon. The index of circularity was determined for each Haversian canal and osteon using the image analysis software program formula:

$$\text{Circularity} = 4\pi\,(\text{area}/\text{perimeter}^2)$$

and was measured on a scale from zero to one, one being a perfect circle. All data collection with the image analysis software was accomplished on a personal computer using the public domain NIH Image program (developed at the U.S. National Institutes of Health and available on the Internet at http://rsb.info.nih.gov/nih-image/).

Only osteons exhibiting circular Haversian canals were selected for analysis to ensure that the osteons measured were not sectioned or polished obliquely, which would obscure the actual circularity. Haversian canals were considered to be appropriately circular for this study if measured to be 0.9 or greater. Osteons that were in the process of being (or had already been) resorbed or replaced were excluded from the study if <85% of the cement line was visible, as were drifting osteons (8) (Fig. 3). The 12 circularity readings from each sample were then averaged to obtain one circularity measurement for each bone sample.

Statistics

Before making a comparison between all human and all nonhuman samples, homogeneity was tested for within each group. A univariate analysis of variance (ANOVA) was performed to establish whether significant differences in osteon circularity exist between sexes and bone type for human samples, and between nonhuman species and nonhuman bone type. Correlation between the bone types for individuals from the human group was also tested. Based on these results, a univariate ANOVA was conducted to detect differences between a pooled sample of human and nonhuman bone. Finally, a discriminant function was performed to test the predictive power of these findings.

Results

Humans

The human sample consisted of seven females and seven males ($n = 14$), and all three bones were used from each individual with the exception of one female rib with extremely thin cortical bone ($n = 41$) (Table 1). Mean osteon circularity for males was 0.851

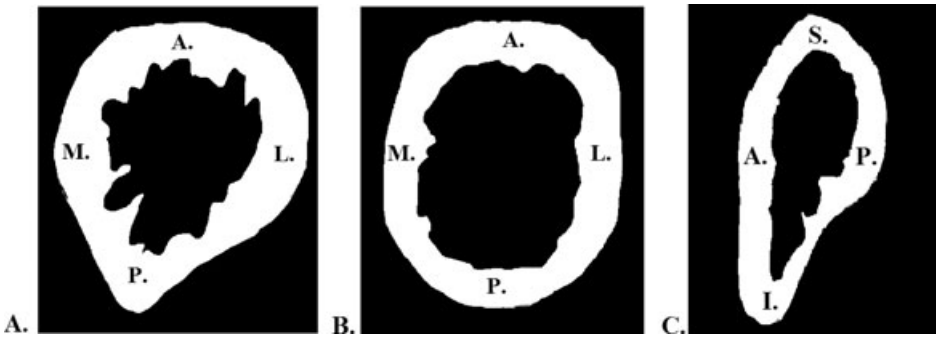

FIG. 2—*A. Anterior (A), posterior (P), medial (M), and lateral (L) areas of femoral cortical bone measured. B. Anterior (A), posterior (P), medial (M), and lateral (L) areas of humeral cortical bone measured. C. Anterior (A), posterior (P), superior (S), and inferior (I) areas of rib cortical bone measured.*

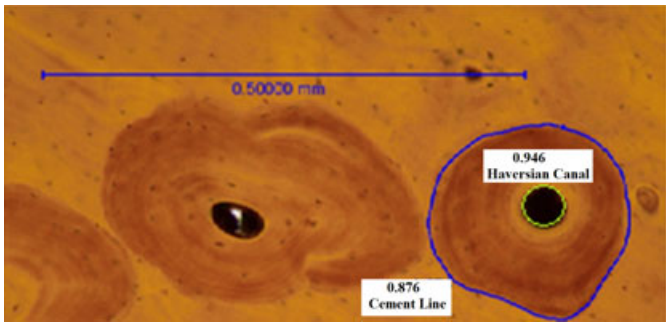

FIG. 3—*Osteon from a* Canis *femur matching criteria for data collection: Type I osteon not in the process of formation or resorption and with a circular Haversian canal (0.946).*

TABLE 2—*Descriptive statistics for human sample (n = 41).*

Human	Mean Osteon Circularity	Standard Error	Lower Range	Upper Range
Female	0.851	0.003	0.845	0.857
Male	0.849	0.003	0.843	0.855
Bone type				
Femur	0.847	0.004	0.837	0.852
Humerus	0.844	0.004	0.837	0.852
Rib	0.859	0.004	0.852	0.867
Cumulative	0.850	0.002	0.837	0.867

TABLE 3—*Results of test for heterogeneity for slopes of ANOVA for human sample with osteon circularity as dependent variable (n = 41).*

Factor	Sum of Squares	*F*-Ratio	*p*-Value
Human			
Sex	0.000037	0.201	0.657
Bone type	0.002	4.700	0.016
Sex*bone type	0.001	1.874	0.169

and 0.849 for females, with a standard error of 0.003 for both sexes (Table 2). Equal variance was determined between the sexes by a Levene's test of equality of variances. An ANOVA revealed an *F*-statistic of 0.201 with a $p = 0.657$ (Table 3), indicating that there is no statistically significant difference between male and female osteon circularity (Table 2).

Mean human osteon circularity for the femur was 0.847, 0.844 for the humerus, and 0.859 for the rib (Table 2). An ANOVA revealed an *F*-statistic of 4.7 with a $p = 0.016$, suggesting that a statistically significant difference was present among at least two of the three bone types (Table 3). A *post hoc* test, least significant difference (LSD), was conducted to determine where differences existed and the results indicate that rib osteon circularity differs significantly from femoral osteon circularity ($p = 0.028$) and humeral osteon circularity ($p = 0.007$), with a standard error of 0.005 for both.

An interaction between sex and bone type was tested for but revealed no statistically significant difference ($p = 0.169$) (Table 3), and osteon circularity of the three bone types does not correlate within the same individual in humans (*p*-values range from 0.640 to 0.876) (Table 4). The mean osteon circularity for the collective human sample was 0.850, with a standard error of 0.002, a lower range of 0.837, and an upper range of 0.867 (Table 2). Variation between the 14 individuals was quantified by running the univariate ANOVA between bone types and box plots, the Levene's test indicating equal variation and box plots demonstrating comparable means for all tests. The observed versus predicted graphs showed no pattern and supports the homogeneity of variance assumption, while the P–P plot of the residuals shows a close relationship between expected and observed values, indicating that the assumptions of normality were correct.

TABLE 4—*Pearson's correlations between bone type and individual by bone indicator.*

Indicator	*r*-Value	*p*-Value
Femur		
Humerus	0.046	0.876
Rib	0.143	0.640
Humerus		
Femur	0.046	0.876
Rib	0.054	0.860
Rib		
Femur	0.143	0.640
Humerus	0.054	0.860

Nonhumans

The nonhuman sample consisted of five specimens each from *Canis*, *Sus*, and *Odocoileus* ($n = 15$), and all three bone types were used with the exception of one *Sus* humerus ($n = 44$) (Table 1). Mean osteon circularity for *Canis* was 0.874, 0.870 for *Sus*, and 0.871 for *Odocoileus* with a standard error of 0.002 for all species (Table 5). An ANOVA revealed an *F*-statistic of 0.602 with a $p = 0.553$ for species differences, suggesting that there is no statistically significant differences between *Canis*, *Sus*, and *Odocoileus* osteon circularity (Table 6).

Mean osteon circularity for the all nonhuman femora was 0.867, 0.870 for nonhuman humeri, and 0.877 for nonhuman ribs (Table 5). ANOVA revealed an *F*-statistic of 4.973 with a *p*-value of 0.013, suggesting that a statistically significant difference was detected in at least two of the three bone types (Table 6). A *post hoc* test, LSD, was conducted to determine where differences existed; its results indicate that rib osteon circularity significantly differed from femoral osteon circularity ($p = 0.004$), but not from humeral osteon circularity ($p = 0.071$), with a standard error of 0.003 for both.

TABLE 5—*Descriptive statistics for nonhuman sample (n = 44).*

Nonhuman	Mean Osteon Circularity	Standard Error	Lower Range	Upper Range
Canis	0.874	0.002	0.869	0.878
Odocoileus	0.871	0.002	0.866	0.875
Sus	0.870	0.002	0.865	0.875
Bone type				
Femur	0.867	0.002	0.867	0.872
Humerus	0.870	0.002	0.865	0.875
Rib	0.877	0.002	0.872	0.882
Cumulative	0.871	0.001	0.865	0.882

TABLE 6—*Results of test for heterogeneity for slopes of ANOVA for nonhuman sample with osteon circularity as dependent variable (n = 44).*

Factor	Sum of Squares	*F*-Ratio	*p*-Value
Nonhuman			
Species	0.000	0.602	0.553
Bone type	0.001	4.973	0.013
Species*bone type	0.000	1.291	0.292

TABLE 7—*Results of test for heterogeneity for slopes of ANOVA between human and nonhuman samples with osteon circularity as dependent variable (n = 41).*

Factor	Sum of Squares	*F*-Ratio	*p*-Value
Human versus nonhuman	0.009	63.912	<0.001

An interaction between species and bone type was tested, but no statistically significant difference emerged ($p = 0.292$) (Table 6), and mean osteon circularity for the collective nonhuman sample was 0.871, with a standard error of 0.001, a lower range of 0.865, and an upper range of 0.882 (Table 5). Box plots demonstrated equal variation and comparable means for all tests. The observed versus predicted graphs showed no pattern and supports the homogeneity of variance assumption, while the P–P plot of the residuals shows a close relationship between expected and observed values, indicating that assumptions of normality were correct.

Human versus Nonhuman

Even though circularity differences were detected among bone types in both human and nonhuman groups, a univariate ANOVA was conducted on pooled samples of both. The results revealed an *F*-statistic of 63.912 and a $p < 0.001$ (Table 7), suggesting a statistically significant difference between pooled human and pooled nonhuman osteon circularity. Box plots demonstrated equal variation, with some overlap of boxes, and comparable means (Fig. 4) for all tests. Concerns about the effect of an autocorrelation are unnecessary because of many of the results and factors listed earlier: no correlation was revealed between bone types of individual humans and all bone samples of deer and pig were not from the same animal. Therefore, an inflated significance from the pooled samples is of no concern, and assumptions are accounted for.

A predictive model with a 76.5% correct classification success rate was created based on the results of this study and is as follows:

Species = (79.473*osteon circularity)−68.435

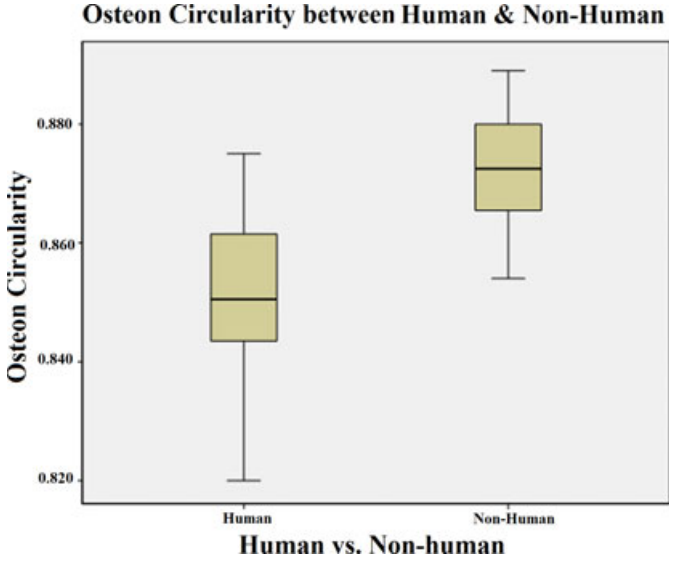

FIG. 4—*Box plot demonstrating comparable osteon circularity means between humans (0.850) and nonhumans (0.871).*

where any result less than zero is most likely human and any result greater than zero is most likely nonhuman.

Intra-Observer Error

Data were re-collected for a total of eight slides on three separate occasions with at least a week between each data collection. Osteon circularity measurements were collected and averaged following the methods of this study. ANOVA revealed an *F*-statistic of 0.374 with a *p*-value of 0.692, and a paired-samples correlation revealed that all trials were highly correlated; therefore, intra-observer error is not of concern. The ImageJ analysis software was also tested to ensure that the program measured circularity was measured accurately (39). This was accomplished by outlining known perfect circles and measuring their circularity with the software. Circularity measurements for all circles ranged from 0.95 to 1.00, all within the acceptable range of a perfect circle as defined by this study. The range of measurements for the perfect circle readings is attributed to the pixilation of the images that the software incorporated into its circularity measurement.

Discussion

To interpret the results of this study and to apply them to differentiate human and nonhuman bone fragments, it is important to identify variables other than species differences that can significantly affect osteon circularity.

Because no statistically significant difference was found between males and females, it does not appear that sex plays a role in osteon circularity (at least in this modern population sample), unlike other aspects of osteon morphology (20–22). Males and females tend to have osteons with similar circularity measurements for all three bone types tested. This suggests that when bone is fragmented, the sex of the individual does not need to be known (and cannot be determined) when distinguishing between human and nonhuman bone.

Species differences among the nonhuman groups were also nonexistent. *Canis*, *Sus*, and *Odocoileus* have remarkably similar osteon circularity measurements with no statistically significant differences detected. These results, however, should not be interpreted to mean that all nonhumans have higher osteon circularity measurements than humans do. This study specifically looked *only at these three species* as they are the most commonly recovered in archeological and forensic cases reported (4). These results indicate that if fragmented bone belonged to one of these three species, it is not necessary to identify the species in order to classify the fragmented bone as human or nonhuman when using this method.

Bone type within both human and nonhuman groups may at first appear to be an important variable when distinguishing between human and nonhuman bone, but when given a closer look, the differences between human and nonhuman osteon circularity are so great that the intraskeletal differences are outweighed. To be sure that knowing bone type is unnecessary when determining if fragmented bone is human or nonhuman, a correlation of osteon circularity was measured between bone types for all individuals but revealed no correlation. These results suggest that osteon circularity does not appear to aid in separating comingled remains because different bones of the same individual can exhibit different circularities. This lack of correlation also ensures that the ANOVA conducted between the pooled samples of humans and nonhumans does not have an over-inflated *p*-value because of autocorrelation within the human sample, thus validating results.

The *p*-value of the ANOVA conducted between the human and nonhuman samples is also not inflated because of the differences in bone types in the nonhuman sample. This is because for most of the nonhuman sample, bones were collected from multiple specimens and not one animal is fully represented by a femur, humerus, and rib set. There can be no correlation then between any of the bone types and one animal; therefore, autocorrelation is of no concern and the nonhuman pooled sample would not inflate the *p*-value of the final ANOVA.

Based on the last ANOVA conducted there appears to be a definite difference between human and nonhuman (*Canis*, *Sus*, and *Odocoileus*) osteon circularity for the femora, humeri, and ribs. Mean human osteon circularity is consistently lower (0.850) than nonhuman circularity (0.871), an apparent trend for all bone types. As a result of these findings, a predictive model, using only osteon circularity, was developed that correctly classifies samples 76.5% of the time. As with most models, there are certain limitations to this model. First, the model was developed using an older human population, with no middle or young adults represented. The nonhuman sample is also limited to three species and does not encompass all nonhumans encountered in both archeological and forensic cases. The model is also based on at least 12 osteon circularity measurements per bone sample: fewer measurements may result in a less accurate classification. Moreover, the circularity difference between human and nonhuman osteons is only 2%, which attests to the critical importance of skilled, accurate measurments by trained researchers. These limitations need to be kept in mind when using the model and assessing the results.

Finally, some findings in this study warrant further research. A comparison of osteon circularity between young, middle, and old adults would substantially contribute to the findings as well as add to our knowledge about age and its effects on osteon circularity. This study would also benefit from a larger and more diverse sample of nonhuman species to better understand differences, or lack thereof, between nonhumans and humans. The most interesting aspect of this study that requires further research concerns the differences in osteon circularity between bone types, more specifically the differences found between long bone and ribs in both of the human and nonhuman samples, and whether or not this reflects their different biomechanical environments, especially relating to modes of locomotion, or differences in metabolic rates.

Conclusion

After reviewing multiple studies that examine variation in the number, size, diameter, and area of osteons as well as Haversian canals, it has become clear that one area of osteon morphology has yet to be looked at critically: osteon circularity. The few studies that consider osteon circularity have not excluded osteons that would skew a normal distribution or in some cases do not have an adequate human sample or nonhuman sample. The findings reported in this study are relevant and significant to the archeology and forensic anthropology fields because they offer a possible new tool when dealing with fragmented remains. Osteon circularity can be used as a complementary tool to DNA and other differentiating techniques and is a relatively cheap process when compared to obtaining a DNA profile. Fragmented bone that was once beyond classification based on macroscopic structures may now be classified using microscopic structures, opening the door to more complete investigations and interpretations of forensic cases or archeological sites.

Acknowledgments

AC would like to acknowledge the University of Indianapolis, Department of Biology for all cadavers used to retrieve human samples, The Ohio State University Veterinary Clinical Sciences for donating all dog samples, and Knightstown Meat Locker (Knightstown, Indiana) for donating all pig and deer samples. AC would also like to thank Dr. Stephen P. Nawrocki, Archeology and Forensic Laboratory Director, University of Indianapolis, and Dr. Nadjib Bouzar, Statistics Professor, University of Indianapolis, for their guidance in my statistical analysis. Finally, AC would like to thank her thesis committee: Dr. Christopher W. Schmidt, Professor and Director of the Indiana Prehistory Laboratory, University of Indianapolis; Dr. Sam D. Stout, Professor, The Ohio State University; and Dr. Gregory A. Reinhardt, Anthropology Department Chair and Professor, University of Indianapolis, for all their guidance and time.

References

1. Stout SD. Histological structure and its preservation in the ancient bone. Curr Anthropol 1978;19(3):601–4.
2. Hillier ML, Bell LS. Differentiating human bone from animal bone: a review of histological methods. J Forensic Sci 2007;52(2):249–63.
3. Cattaneo C, Porta D, Gibelli D, Gamba C. Histological determination of human origin of bone fragments. J Forensic Sci 2009;54(3):1–3.
4. Morris ZH. Quantitative and spatial analysis of the microscopic bone structures of deer, dog, and pig [Master's Thesis]. Baton Rouge (LA): Louisiana State University, 2007.
5. Vajda EG, Kneissel M, Muggenburg B, Miller SC. Increased intracortical bone remodeling during lactation in beagle dogs. Biol Reprod 1999;61:1439–44.
6. Martin RB, Burr DB, Sharkey NA. Skeletal tissue mechanics. New York, NY: Springer, 1998;36–40.
7. Ortner DJ. Identification of pathological conditions in human skeletal remains, 2nd edn. San Diego, CA: Academic Press, 2003.
8. Robling AG, Stout SD. Morphology of the drifting osteon. Cell Tissue Organs 1999;164:192–204.
9. Pettit AR, Chang MK, Hume DA. Osteonal macrophages: a new twist on coupling during bone dynamics. Bone 2008;43:976–82.
10. Parfitt AM. Targeted and nontargeted remodeling: relationship to basic multicellular unit organization and progression. Bone 2005;30(1):5–7.
11. Robling AG, Castillo AB, Turner CH. Biomechanical and molecular regulation of bone remodeling. Annu Rev Biomed Eng 2006;8:455–98.
12. van Oers R. A unified theory for osteonal and hemi-osteonal remodeling. Bone 2008;42(2):250–9.
13. Currey JD. Bones: structure and mechanics. Princeton, NJ: Princeton University Press, 2002.
14. Skedros JG, Holmes JL, Vajda EG, Bloebaum RD. Cement lines of secondary osteons in human bone are not mineral-deficient: new data in a historical perspective. Anat Rec 2005;286A(1):781–803.
15. Stout SD, Crowder C. Bone remodeling, histomorphology and histomorphometry. In: Crowder C, Stout SD, editors. Bone histology: an anthropological perspective. Boca Raton, FL: CRC Press, 2011;1–22.
16. Cooper RR, Milgram JW, Robinson RA. Morphology of the osteon: an electron microscopic study. J Bone Joint Surg 1966;48(7):1239–72.
17. Qui S, Fyhrie DP, Palnitkar S, Rao SD. Histomorphometric assessment of haversion canal and osteocyte lacunae in different-sized osteons in human rib. Anat Rec A Discov Mol Cell Evol Biol 2003;272A:520–5.
18. Pirock DJ, Ramser JR, Takahashi H, Villaneuva AR, Frost HM. Normal histological, tetracycline and dynamic parameters in human, mineralized bone section. Henry Ford Hosp Med J 1966;14:195–218.
19. Thompson DD. Age changes in bone mineralization, cortical thickness and Haversian canal area. Calcif Tissue Int 1980;31:5–11.
20. Britz HM, Thomas CDL, Clement JG, Cooper DML. The relation of femoral osteon geometry to age, sex, height, and weight. Bone 2009;45:77–83.
21. Burr DB, Ruff CB, Thompson DD. Patterns of skeletal histologic change through time: comparison of an Archaic Native American population with modern populations. Anat Rec 1990;226:307–13.

22. Mulhern DM, Van Gerven DP. Patterns of femoral bone remodeling dynamics in a Medieval Nubian population. Am J Phys Anthropol 1997;104:133–46.
23. Pfeiffer S. Variability in osteon size in recent human populations. Am J Phys Anthropol 1998;106(2):219–27.
24. Manson JD, Waters NE. Assessment of the osteon maturation rate in dog. Arch Oral Biol 1967;12:1577–91.
25. Harris WH, Haywood EA, La Vorgna J, Hamblen DL. Spatial and temporal variations in cortical bone formation in dogs: a long-term study. J Bone Joint Surg 1968;50:1118–28.
26. Hidek S, Matsumoto M, Ohsako S, Toyoshima Y, Nishinakagawa H. A histometrical study of long bones of raccoon dogs, Nyctereutes procyonoides and badgers, Meles meles. J Vet Med Sci 1998;60(3):323–6.
27. Georgia R, Albu I, Sico M, Georoceanu M. Comparative aspects of density and diameter of Haversian canals in the diaphyseal compact bone of man and dog. Morphol Embryol (Bucur) 1982;28(1):4–11.
28. Albu I, Georgia R, Georoceanu M. The canal system in the diaphyseal compact bone of the femur in some mammals. Ann Anat 1990;170(3/4):181–7.
29. Mulhern DM, Ubelaker DH. Differences in osteon banding between human and nonhuman bone. J Forensic Sci 2001;46:220–2.
30. Mori R, Kodaka T, Soeta S, Sato J, Kakino J, Hamato S, et al. Preliminary study of histological comparison on the growth patterns of long-bone cortex in young calf, pig, and sheep. J Vet Med Sci 2005;67(12):1223–9.
31. Mainland I, Schutkowski H, Thomson AF. Macro- and micromorphological features of lifestyle differences in pig and wild boar. Anthropozoologica 2007;42(2):89–106.
32. Owsley DW, Mires AM, Keith MS. Case involving differentiation of deer and human bone fragments. J Forensic Sci 1984;30(2):572–8.
33. Martiniakova M, Grosskopf B, Omelka R, Vondrakova M, Bauerova M. Differences among species in compact bone tissue microstructure of mammalian skeleton: use of discriminant function analysis for species identification. J Forensic Sci 2006;51(6):1235–9.
34. Martiniakova M, Grosskopf B, Omelka R, Dammers K, Vonderakova M, Bauerova M. Histological study of compact bone tissue in some mammals: a method for species determination. Int J Osteoarch 2006;17(1):82–90.
35. Watson J, McClelland J. Distinguishing human from animal bone. Arizona State Museum: Cultural Service Resources, 2009, http://www.statemuseum.arizona.edu/crservices/human_animal_bone.shtml (accessed March 15, 2010).
36. Ubelaker DH. Human skeletal remains, excavation, analysis, interpretation, 3rd edn. Manuals on archaeology 2. Washington, DC: Taraxacum, 1999.
37. Skedros JG, Hunt KJ, Dayton MT, Bloebaum RD, Bachus KN. Relationships of loading history and structural material characteristics of bone: development of the mule deer calcaneus. J Morphol 2004;259:281–307.
38. Anderson C. Manual for examination of bone. Boca Raton, FL: CRC Press, 1982;116.
39. Rasband WS, Image J. Bethesda, MD: U.S. National Institutes of Health, 1997–2011, http://imagej.nih.gov/ij/ (accessed October 30, 2011).

Additional information and reprint requests:
Annamaria Crescimanno, M.S.
249 W El Portal, #4
San Clemente, CA 92672
E-mail: crescimannoa@gmail.com